The EuroBiotech Journal
RESEARCH ARTICLE
NanoBiotechnology

Bioactive Hydrogel for Regenerative Wound Healing: Evaluating Angiogenesis and Toxicity

Devadass Jessy Mercy[1], Gopalarethinam Janani[1], Saranya Udayakumar[1], Agnishwar Girigoswami[1**], Koyeli Girigoswami[2,3*]

Abstract

Scar-free wound healing remains a major challenge in regenerative medicine. In this study, a carboxymethyl cellulose (CMC)-based hydrogel nanocomposite containing silver nanoparticles (CMC@Ag) was developed, along with a phytocompound-enriched variant (CMC@Ag+P) incorporating aloe vera, curcumin, and plantain peel extracts. The phytocompound-infused hydrogel exhibited enhanced antibacterial activity, biocompatibility, and scar-free healing potential, supporting tissue regeneration. An in vitro scratch assay using the A375 cell line showed 89% cell proliferation and migration at high doses and 69% at low doses of CMC@Ag+P. Zebrafish toxicity assays confirmed its safety, with hatchability rates of 82% (low dose) and 71% (high dose). The chorioallantoic membrane (CAM) assay demonstrated strong angiogenic activity, particularly in CMC@Ag+P, indicating improved vascularization essential for tissue repair. Statistical analysis using the Student's t-test revealed significant differences between hydrogel-treated groups and controls ($p < 0.05$), confirming the enhanced healing and scar-minimization effects. Previous animal studies further validated the scar-free wound healing potential of these hydrogel highlighting the synergistic role of phytocompounds in promoting effective tissue regeneration.

Keywords: Burn wounds, Wound healing, Silver nanoparticles, Carboxymethyl cellulose, Bioactive compounds, Nanohydrogel, Angiogensis

Introduction

The chief organ that offers obstruction and protects the body from external harmful diseases and pathogens is the skin. It plays an important role in maintaining the body's integrity, blood clots, and fluids (1). Burn injuries are the most traumatic injury that affects all the body organs and eventually leads to death. Bacterial infection over the wound is a serious disadvantage in the wound care management system if it is not controlled in the case of severe burn wounds, chronic ulcers, traumatic injuries, diabetic wounds, etc. Severe burn wounds sooner or later lead to several organ failures by affecting numerous response mechanisms, and body metabolisms resulting in prolonged trauma (2). It is essential to note that all burn wound management objectives are the same, even though there are many different types of burns. These goals include halting the burning process, alleviating pain, and minimizing scarring thus preventing secondary infections by avoiding future complications (3). Depending on the cause, depth, and severity, burn wounds can be classified into various types, 1st degree as superficial wounds, 2nd degree as superficial partial-thickness wounds, 3rd degree as moderate partial thickness wounds; 4th degree as deep partial-thickness wounds, and 5th-degree full-thickness wounds. There are different phases of wound healing which are mostly promoted by various cells, and biological functions that escape from coinciding, but the right sequence order leads to potential wound healing for specific cases (4).

Despite the development in medical sciences, various limitations continue in the ef-

[1]Medical Bionanotechnology, Faculty of Allied Health Sciences, Chettinad Hospital and Research Institute, Chettinad Academy of Research and Education, Chettinad Health City, Kelambakkam, 603103, Tamilnadu, India
[2]Department of Obstetrics and Gynaecology, Saveetha Medical College and Hospitals, Saveetha Institute of Medical and Technical Sciences, Thandalam, Chennai, 602105, India
[3] Medical Bionanotechnology Lab, Centre for Global Health Research, Saveetha Medical College and Hospital, Saveetha Institute of Medical and Technical Sciences, Thandalam, Chennai, 602105, India

Corresponding authors:
*E-mail (corresponding author): koyelig@gmail.com; koyelig.smc@saveetha.com
**E-mail (co-corresponding author): agnishwarg@gmail.com; dragnishwar@care.edu.in

DOI: 10.2478/ebtj-2026-0003

fective management and treatment of burn wounds which ultimately alters the recovery period, affecting the patient outcomes by decreasing the quality of life. Infection, toxicity, and biofilm formation are some of the most prominent challenges in wound healing because wounds can be easily influenced by bacteria that in turn minimize the healing process by suppressing the inflammatory response mechanism that eventually disturbs tissue regeneration (5, 6). Similarly, limited grafting options and the availability of donors are some critical issues because skin grafting is the standard procedure for burn wound treatment.

However, these grafting techniques used in wound healing treatment limit the availability of donors especially in case of severe burn. It often results in contractures, and scar formation that minimizes the aesthetic outcomes (7, 8). Debriding at an appropriate time reduces the infection and scarring therefore promoting to proliferative phase from the inflammatory phase (9). Initiating treatment for scarring, utilizing silicone sheets, laser therapy, and pressure garments, limits its effects and encompasses for a prolonged period (6). Nerve damage due to burn wounds also results in chronic pain and sensory loss (10). Likewise, local factors, systemic factors like anemia, hypoxia, edema and psychological impacts like trauma, and mental distress, and technological limitations like lack of proper effects of dressings, toxicity, and reliability also limit the healing of wounds (6, 11).

Nanotechnology significantly overcomes these limitations through various advanced materials and drug delivery systems (12). Researchers have developed nanomaterials, and nanostructures that are formulated in this manner, to improve the most essential properties like solubility, bioavailability, biocompatibility, non-toxicity, and increased therapeutic outcomes eventually leading to rapid healing with fewer complications (13). Barkat *et al* developed nanosuspensions loaded with silver sulfadiazine that improves the bioavailability, solubility, and toxicity issues, thus promoting healing of wounds even in lower concentrations (14). Incorporation of rhamnose, a therapeutic and an angiogenic agent along with electrospun nanofiber film results in improved healing activities and initiated 30% rapid wound closure compared to the unincorporated nanofibers (15). Likewise, plant extracts incorporated with nanomaterials significantly played a major role in burn wound healing. Due to the integration of both plant extracts and nanomaterials, various mechanisms can be enhanced like faster healing, promotion of growth response mechanism (anti-inflammatory, antimicrobial, antioxidant, cell proliferation), and increases in therapeutic applications (16). However, the previous literature promoted burn wound healing but limited the scar-free healing.

Wound healing enhancement can happen if the formulation has enhanced antimicrobial effect, enhanced cell migration, and fast blood vessel formation or angiogenesis capacity. In the present study, a multifunctional hydrogel system intergrating the blended carboxymethyl cellulose (CMC) with plant extracts like aloe vera, curcumin, and plantain peel along with silver nanoparticles to address the key difficulties in burn wound healing. Currently, most wound healing treatments concentrates on wound closure but fail to prevent the scarring and other properties. Similarly, there are limited research combining nanomaterials with several plant extracts in a combined, single hydrogel for complete scar-free burn wound healing. Given that other conventional treatments which specifically aim at wound closure, this hydrogel is specifically desgined to promote scar-free wound healing by enhancing the cell migration, biocompatibility, antimicrobial and pro-angiogenic activity on both *in vitro* and *in vivo* models. The combined approach not only improves the healing properties but also promotes tissue regeneration and remodeling, indicating a substantial advancement over pre-existing nanomaterial and plant extract based therapies.

Materials and Methods

2.1 Materials

The fertilized eggs were procured from TANUVAS, Chennai, and A375 cell lines from NCSS, Pune. The zebrafish embryos were procured from a local aquarium. Fetal Bovine Serum was procured from Gibco, USA. Dimethyl sulphoxide, boric acid, and silver nitrate were procured from RANKEM, India. Benzene, orthophosphoric acid, curcumin, and acetic acid were procured from SRL. Dulbecco's Modified Eagle Medium, Antibiotic-antimycotic solution, and sodium carboxymethyl cellulose were procured from HiMedia. The other materials like aloe vera and plantain were procured from Chettinad Organics and the local market.

2.2 Preparation and Characterization of the Hydrogels

2.2.1 Preparation of CMC@Ag hydrogel

The synthesis protocol was selected from previous literature (17), modified and used prior to our laboratory facility which involved dissolving 1 g of NaCMC in 50 ml of distilled water under continuous stirring. Once fully dissolved, 5 ml of 0.1 M silver nitrate solution was added dropwise and the mixture was heated to 95°C until it began to boil. The heating was stopped while the stirring continued for 15 min and the mixture was cooled down to room temperature. 7.5 g of citric acid was added and stirred until dissolved and the it was homogenized using a probe sonicator for 10 min at 40kHz. Then the solution was poured into perti plates (polypropylene), incubated for 24 h at 40°C followed by 80°C for another 24 h. Later the hydrogel embedded with (0.1 M) AgNps was extracted.

2.2.2 Preparation of CMC@Ag+P hydrogel

The CMC@Ag+P hydrogel synthesized in the similar manner, where 1g of NaCMC was dissolved in 50 ml of distilled water containing plantain peel extract, aloe vera extract and curcumin. After complete dissolution, 5 ml of 0.1 M silver nitrate was added dropwise and heated to 95°C until boiling, and stirred for 15 min. It was then cooled down to room temperature and 7.5 g of citric acid was added. Further, it was homogenized using a probe sonicator for 10 min at 40kHz. Then the

solution was poured into perti plates (polypropylene), incubated for 24 h at 40°C followed by 80°C for another 24 h. Later the hydrogel embedded with (0.1 M) AgNps with the plant extracts was extracted. Finally, the extracted CMC@Ag+P hydrogel contains, 0.1 M , 0.0025% of curcumin , 0.25% of both plantain peel and aloe vera extracts, respectively.

2.2.3 Characterization of CMC@Ag and CMC@Ag+P hydrogels

The synthesized hydrogel was characterized using various photophysical tools which was briefly explained in Sofini et al. (18). We synthesized the hydrogels and characterized it after sonication. In this study, SEM was used to observe the surface morphology, DLS, FTIR, and particle size analyzer were used to characterize size and hydrodynamic diameter and zeta potential of both hydrogels, respectively. For SEM analysis, the hydrogel was air dried in a closed box above a thin grease free clean glass slide and subjected to SEM analysis after gold and palladium alloy coating using FEI Quanta FEG 200-High Resolution Scanning Electron Microscope (SEM). For DLS and zeta potential, the samples were diluted 10 times using PBS, and subjected to hydrodynamic diameter and zeta potential measurement using Malvern zeta sizer. To prepare FTIR samples, only CMC, CMC@Ag, and CMC@Ag+P hydrogels, were dried completely at 40 °C using a hot air oven, crushed using a mortar pestle and KBr pellet was made. Bruker alpha FTIR instrument was used to identify the peaks for only CMC, CMC@Ag, and CMC@Ag+P hydrogels hydrogels in transmittance mode.

2.3 Cell migration assay

A cell migration assay was conducted using the A375 cell line to evaluate the wound-healing effects of the synthesized hydrogels as per our recent study (19). The cells were cultured according to standard laboratory protocols (DMEM that contained 10 % FBS and antibiotics at 1 % concentration, maintained in a CO_2 incubator), and the scratch was manually created using a sterile tip over the cell monolayer cultured in 35 mm Petri plates. Treatment was provided using two different hydrogel concentrations over a period of four days (CMC@Ag and CMC@Ag+P at high (2.5 µg/ml) and low (1.25 µg/ml) concentrations). Photographs were taken every day to monitor the wound healing process, and the percentage of wound closure was determined finally by Magnus software as described earlier (19).

2.4 *In vivo* biocompatibility assay

The *in vivo* biocompatibility study utilizing the zebrafish embryos provides the vital knowledge on the toxicity analysis and developmental safety of our formulated hydrogel. Moreover these embryos are widely used due to its transparent nature, rapid growth and has the well-maintained genetic pathways involved in wound healing and tissue regeneration. The toxicity study was performed after the IAEC approval (IAEC2/Proposal:118/A.Lr:90/Dt:16.09.2023) from the Institutional Animal Ethics Committee, Chettinad Academy of Research and Education. Zebrafish embryos were used as an in vivo model to evaluate the toxicity of the hydrogels. A total of 60 embryos were utilized, with 10 embryos allocated to each treatment group, including the control. Photograph of 10 hours post-fertilization (hpf) was taken and treatment was provided (CMC@Ag and CMC@Ag+P at high (2.5 µg/ml) and low (1.25 µg/ml) concentrations), covered, and kept in dark. Further, the morphological changes were analyzed using optical microscopy, and photographs were taken at 28, 52, and 76 hpf. Finally, the % of cumulative hatchability was also calculated and plotted (20).

2.5 Evaluating the potential angiogenesis activity on CAM membrane

The CAM assay was conducted to evaluate the vascular response, chick viability, angiogenic potential, biocompatibility, and tissue formation associated with the hydrogels. Fertilized eggs incubated for 48 hours were procured before the experiment and maintained at 37°C with 60% humidity. The eggshell surface was sanitized using 70% ethanol, and the CAM layer was marked. About 1 cm^2 vent was carefully created on the eggshell, vitality was checked with the help of a mobile torch light and then the shell was disinfected, sealed with sterile tape, and incubated inside an egg incubator maintained at 37 °C. On the second day, treatment was administered by placing a sterile filter disc on the membrane and the procedure was conducted inside a biosafety cabinet in a sterile environment. Before application, the hydrogels were filtered and diluted with phosphate-buffered saline (PBS). The dilution is done according to the dose of treatment (2.5 µg/ml and 1.25 µg/ml) in PBS, and from the diluted stock, 10 µl is added on the sterile disc. After treatment, the opening was disinfected sealed under sterile conditions, and further incubated.

A total of 21 fertilized eggs were divided into six groups, each consisting of three eggs. Group 1 served as the positive control and was treated with heparin (PC), while Group 2 was an untreated control (UC) group. Group 3 and Group 4 received high (2.5 µg/ml) and low (1.25 µg/ml) concentrations of CMC@Ag, respectively, whereas Group 5 and Group 6 were treated with high (2.5 µg/ml) and low (1.25 µg/ml) concentrations of CMC@Ag+P. The eggs were incubated under the same humidity conditions until day five. On the fifth day, the eggs were opened, and the CAM membrane was observed and photographed. Morphological analysis of the fertilized eggs was performed using the IKOSA software, followed by statistical analysis, which was presented in a graphical format.

2.6 Statistical Analysis

Statistical analysis was performed between the experimental samples and control groups using the Student's t-test. The analysis was carried out for both the concentrations of CMC@Ag and CMC@Ag+P (1.25 µg/ml and 2.5 µg/ml) as well as for positive control (Heparin) and negative control. The p-value of less than 0.05 was considered statistically significant and the significance compared between positive control and both hydrogels was denoted as ***-p <0.01; **-p <0.02; *-p <0.05 and significance compared between negative control and both hydrogels

was denoted as α-$p < 0.01$; β-$p < 0.001$, respectively.

Results and Discussion

3.1 Prepartion and Characterizations of the hydrogels

The hydrogels was prepared following the protocol of Sofini et al (18). The plant extracts and hydrogels characterized previously provided the UV absorption range at 277 nm for plantain peel, 307 nm for aloe vera, 420 nm for curcumin, 416 nm for hydrogel with only silver and 446 nm for hydrogel with silver and plant extracts. Similarly the size and zeta potential for the hydrogel with only silver was found to be 430 nm and -2.18 mV and hydrogel with silver + plant extracts was 375 nm and -2.88 mV respectively. The corresponding chemical bonds was studied using FT-IR. Chemical groups like carboxylic acids, alkenes, aliphatic amines, alkyl halides identified for aloe vera. Functional groups like alcohols, phenols, alkynes, alkyl halides and aliphatic amines are some identified for plantain peel and for curcumin the functional groups like, alcohols, phenols, nitriles, aromatics, aliphatic amines and alkyl halides are identified for curcumin solution. All the above functional groups along with aldehydes, primary amines and α,β unsaturated ethers was identified in both hydrogels. The physicochemical constituents of both extacts was analyzed by GC-MS and the chemical constituents inducing scar-free wound healing was found. The chemical constituents in plantain peel extract "Cholesta-8,24-dien-3-ol, 4-methyl-,(3.beta.,4.alpha.)" and in aloe vera "Pyrogallol, 3TBDMS derivative" promoted scar-free wound healing thus proving the healing efficacy of the hydrogel CMC@Ag+P (18).

In our current study, we freshly prepared the hydrogels, which were subjected to additional 10 min sonication to ensure the proper dispersion of the particles. This resulted in a slight decrease of the particle's hydrodynamic diameter and increase in the zeta potential of both the hydrogels. Table 1 represents the size and zeta potential of both the hydrogels. The results indicate that there was an increase in size after the incorporation of the plant extracts and the zeta potential indicated a high stability of our formulation, both CMC@Ag and CMC@Ag+P. The PDI was below 0.5 indicating a homogenous formulation. Fig 1 shows the surface morphology of the hydrogel CMC@Ag (Fig 1. a) and CMC@Ag+P (Fig 1. b). The CMC@ Ag hydrogel has a crisscross morphology with the components in the shape of needles, whereas, for the hydrogel CMC@Ag+P, the morphology is like a bunch of begonia flowers. The size as visualized from the SEM image is also reduced for CMC@Ag+P compared to CMC@Ag.

The FTIR peaks of only CMC, CMC@Ag, and CMC@Ag+P is shown in Figure 2. The corresponding peaks and their respective bond stretching, bending and vibrations are listed in Table 2. It is clearly seen that there is a shift in the respective peaks of CMC@Ag for CMC@Ag+P, illustrating that the phytochemicals are incorporated in the structure of the CMC hydrogel and the respective bonds have been stretched or compressed.

3.2 Cell migration Assay

Fig 3 reveals the cell migration or wound healing activity of both the hydrogels. The high cell migration was promoted due to the combination of extracts with CMC along with AgNPs. Despite AgNPs, the aloe vera extract naturally soothes the wound environment reducing the irritation and plantain peel extract controls the pathogens offering antibacterial properties and initiates the re-epithelization period by improving the scar area. The curcumin enriched with antioxidant, antibacterial, and anti-inflammatory properties supports the regeneration of tissues, by decreasing inflammation and protects the wound area from infections. Hence the combination of these along with CMC and AgNps promotes the essential and effective cell migration or burn wound healing. Table 3 shows the wound closure percentage assessed using Magnus software for the different groups. It was evident that more than 80 % of the wound was closed for high-dose exposure to CMC@Ag+Pcompared to only 37 % healing for CMC@Ag at a high dose (2.5 µg/ml). In untreated control cells, the healing was nearly 35 % which was enhanced 2.2-fold when the cells were treated with our engineered hydrogel, CMC@Ag+P. This supports the rapid cell-cell communication and migration of cells after exposure to CMC@Ag+P, which is an important requisite for wound healing.

Table 1. Presents the hydrodynamic diameter and zeta potential measured for both hydrogels.

Hydrogels	Hydrodynamic diameter (nm)	Poly Dispersity Index (PDI)	Zeta Potential (mV)
CMC@Ag	344	0.209	-37.3
CMC@Ag+P	352	0.328	-35.9

3.3 *In vivo* toxicity assay

The zebrafish embryo was used as an *in vivo* model to analyze the toxicity due to its transparency, speedy growth, and simple observation. The toxicity of both hydrogels was measured by observing the morphological changes seen in the embryos (Fig

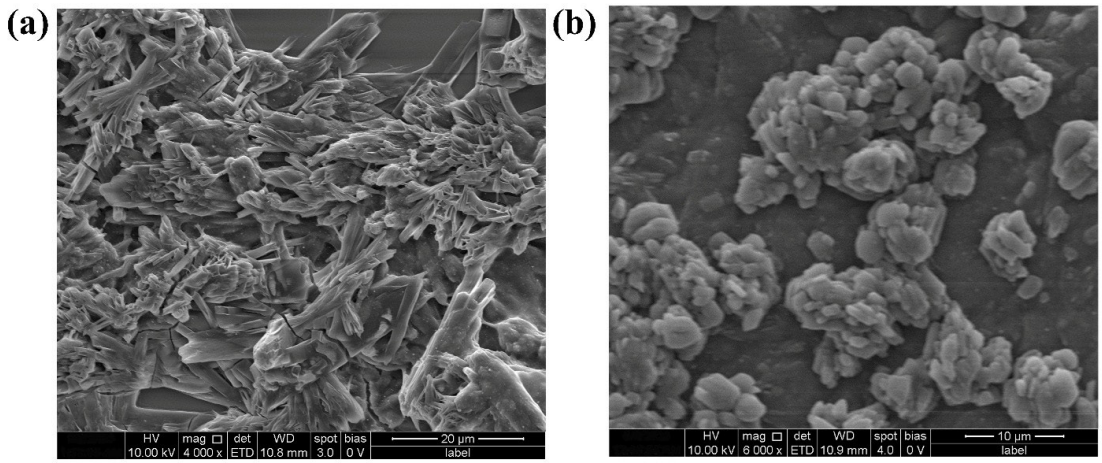

Figure 1. The scanning electron micrographs showing the surface morphology of both (a) CMC@Ag and (b) CMC@Ag+P.

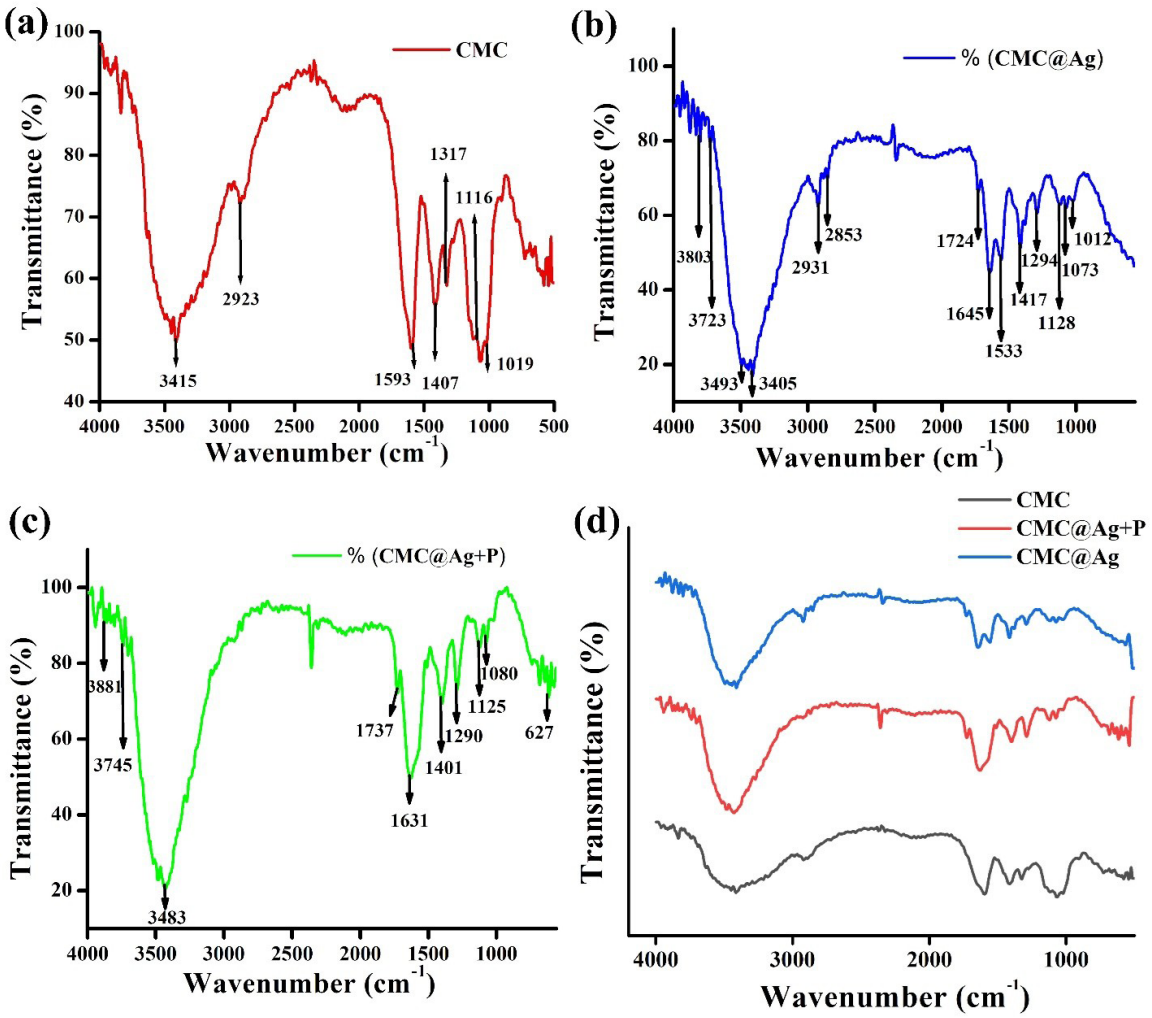

Figure 2. The FTIR spectra for (a) only CMC, (b) CMC@Ag, and (c) CMC@Ag+P. The stacked FTIR spectra for all the three compounds is shown in (d) for comparing the peak shifts.

Table 2. The respective bonds present in the samples revealed from the FTIR peaks of only CMC, CMC@Ag, and CMC@Ag+P.

CMC@Ag		
Wavenumber	**Chemical bond**	**Functional groups**
3803	O-H Stretch, free hydroxyl	Alcohols, phenols
3723	O-H Stretch, free hydroxyl	Alcohols, phenols
3405	N-H Stretch, O-H Stretch, H- bonded	1°, 2° amines, alcohols, phenols
2931	C-H Stretch	Alkanes
2853	C-H Stretch	Alkanes
1724	C=O Stretch	α, β- unsaturated aldehydes, ketones
1645	N-H Bend	1° amines
1533	N-O asymmetric Stretch	Nitro compounds
1417	C-C Stretch in ring	Aromatics
1294	C-H wag ($-CH_2X$)	Alkyl halides
1128	C-N Stretch	Aliphatic amines
1073	C-N Stretch	Aliphatic amines
1012	=C-H Bend	Alkenes
CMC@Ag+P		
Wavenumber	**Chemical bond**	**Functional groups**
3889	O-H Stretch, free hydroxyl	Alcohols, phenols
3745	O-H Stretch, free hydroxyl	Alcohols, phenols
3483	N-H Stretch	1°, 2° amines, alcohols, phenols
1737	C=O Stretch	Aldehydes, saturated aliphatic
1631	N-H Bend	1° amines
1401	C-C Stretch in ring	Aromatics
1290	C-H wag ($-CH_2X$)	Alkyl halides
1125	C-N Stretch	Aliphatic amines
1080	C-N Stretch	Aliphatic amines
627	C-Cl Stretch	Alkyl halides
PURE CMC		
Wavenumber	**Chemical bond**	**Functional groups**
3415	O-H Stretch, H-bonded	Alcohols, phenols
2923	O-H Stretch, free hydroxyl	Alcohols, phenols
1593	N-H Bend	1° amines
1407	C-C Stretch in ring	Aromatics
1317	C-N Stretch	Aromatics amines
1167	C-H wag ($-CH_2X$)	Alkyl halides
1019	C-O Stretch	Alcohols, carboxylic acids, esters, ethers
1080	C-N Stretch	Aliphatic amines
627	C-Cl Stretch	Alkyl halides

4. a). The group treated with both concentrations of CMC@Ag+P (1.25 µg/ml and 2.5 µg/ml) showed normal development similar to untreated control groups, whereas the group treated with CMC@Ag at the same concentrations showed developmental abnormalities due to possible toxic effects, as evidenced by delayed growth and morphological changes. Furthermore, the cumulative hatchability percentage (%) was also determined for both hydrogels till 72 hpf and plotted as a graph (Fig 4. b). The graph clearly shows the percentage of hatchability was higher in both concentrations of CMC@Ag+P than CMC@Ag, even in 72 hpf. Delayed hatching was also observed for the CMC@Ag group at a high dose (2.5 µg/ml), whereas all the embryos hatched at the proper time for both high and low doses of CMC@Ag+P, like the untreated control. This clearly indicates that the addition of plant extracts with CMC@Ag decreased the toxicity and increased its biocompatibility contributing to potential biomedical applications.

3.4 CAM Assay for Angiogenesis Assessment

The CAM assay indicates higher angiogenic activity in the CMC@Ag+P treated group compared to CMC@Ag and untreated control. The pro-angiogenic activity was observed in

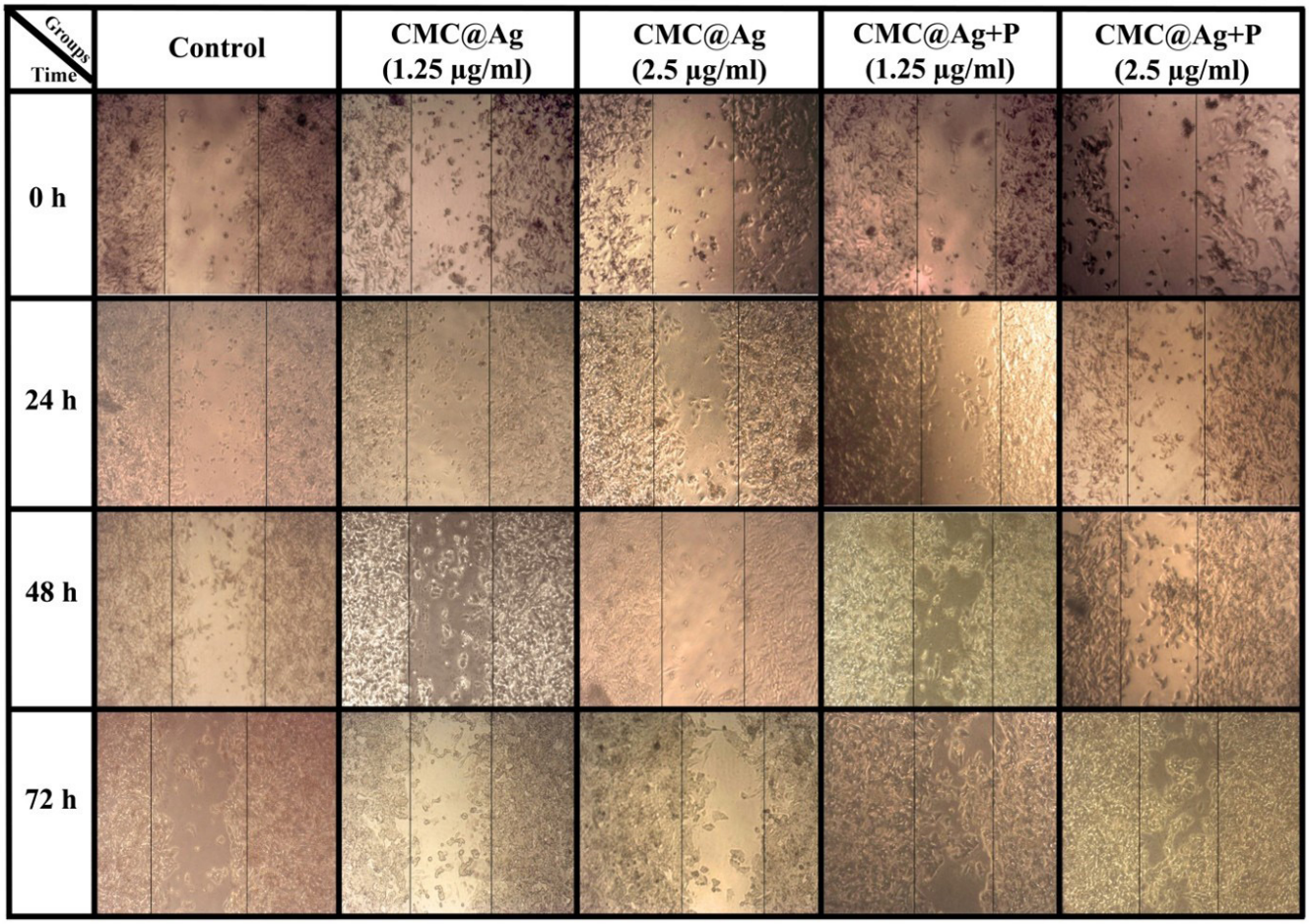

Figure 3. Represents the image panel of cell migration assay showing the progression of wound closure over time

Table 3. The wound closure percentage at 72h for A375 scratch assay estimated using Magnus software.

Treatment groups	Wound closure percentage at 72h
Untreated control	35 ± 2.2
CMC@Ag (1.25 µg/ml)	33 ± 3.1
CMC@Ag (2.5 µg/ml)	37 ± 2.7
CMC@Ag+P (1.25 µg/ml)	66 ± 4.6
CMC@Ag+P (2.5 µg/ml)	82 ± 3.9

both the concentrations of CMC@Ag+P (2.5 µg/ml and 1.25 µg/ml) (Fig 5. c, d), probably due to the synergistic effect of plant extracts along with CMC@Ag stimulating vascular growth. In contrast, both the concentrations of CMC@Ag (2.5 µg/ml and 1.25 µg/ml) (Fig 5. a, b) resulted in decreased vascularization and showed potential toxicity at higher concentrations. Assay validity was confirmed by proving strong angiogenesis with heparin heparin-treated group (Fig 5. d), but standard vascularization remained the same with the untreated control group (Fig 5. e). Ultimately, these results proved that the CMC@Ag+P formulation enhances angiogenesis which can be suitable for burn wound healing applications. This can be further validated by the quantitative and statistical analysis of the CAM assay (Fig. 6). The vessel branching point was significantly higher for both low and high-dose treated CMC@Ag+P compared to CMC@Ag. Regarding the vessel mean thickness, CMC@Ag+P and CMC@Ag, both had a significantly higher capacity to induce vessel thickness compared to positive control heparin. At high doses, CMC@Ag+P could induce significantly lengthier vessels compared to CMC@Ag; even higher than heparin. The vessel total area was also higher in CMC@Ag+P compared to CMC@Ag, for both low and high doses. Overall, the quantitative analysis of the CAM assay indicated that CMC@Ag resulted in lower angiogenic activity, suggesting that silver nanoparticles alone moderately promoted vessel formation. However, CMC@Ag+P could exhibit high angiogenesis capacity that could aid in enhanced wound healing *in vivo*. New blood vessel formation will support the transport of nutrients to the wound site faster thereby enhancing the healing rate.

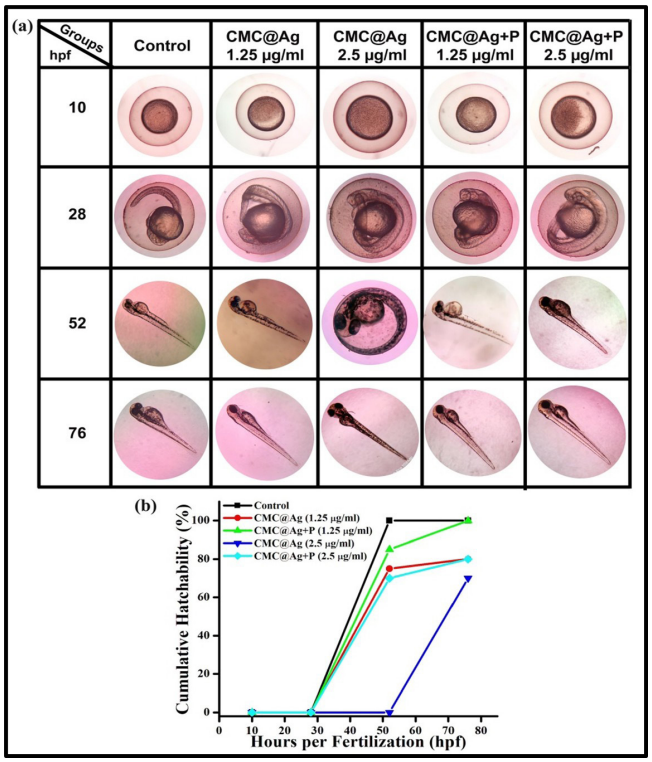

Figure 4. (a) Illustrates the toxicity assessment of CMC@Ag and CMC@Ag+P on Zebrafish; (b) cumulative hatchability percentage (%) of both the hydrogels compared to control.

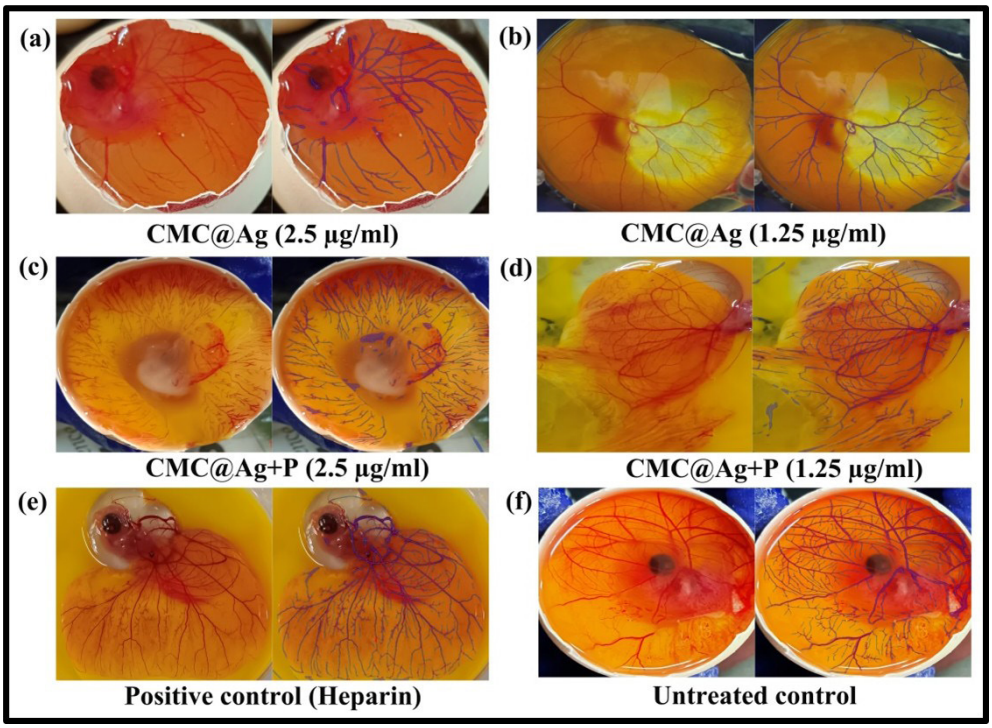

Figure 5. Evaluation of Angiogenic activity using CAM assay. (a, b) CAM membranes treated with high (2.5 µg/ml) and low (1.5 µg/ml) concentrations of CMC@Ag hydrogel; (c, d) CAM membranes treated high (2.5 µg/ml) and low (1.5 µg/ml) concentrations of CMC@Ag+P hydrogel; (e) positive control (Heparin-treated); (f) CAM membrane treated with negative control.

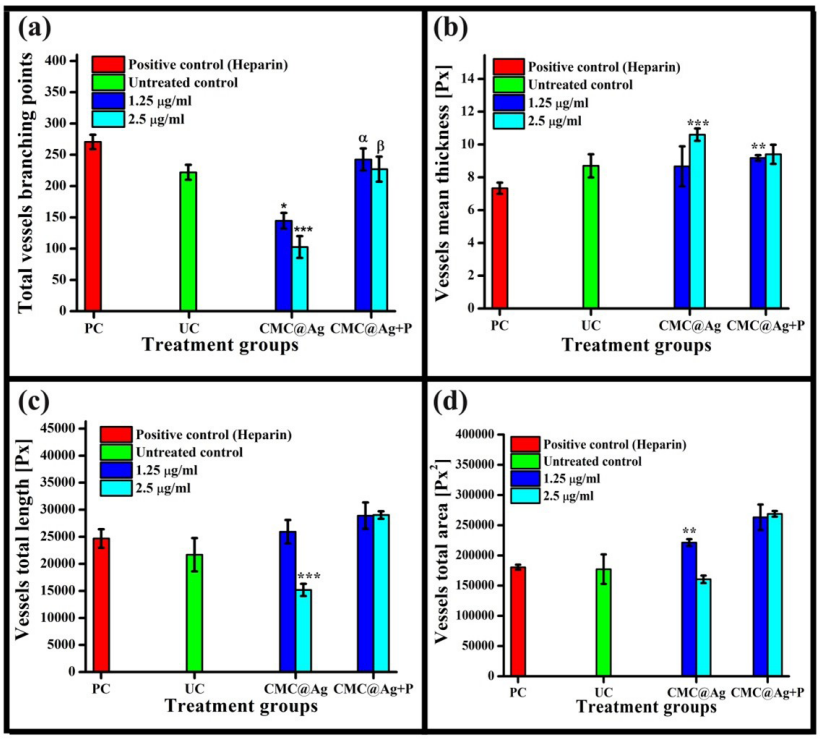

Figure 6. Quantitative analysis of angiogenesis parameters from CAM assay, (a) the number of branching points (b) the number of vessel mean thickness (c) number of vessel length (d) the total area of the vessels. The results are expressed as the mean ± SD. Statistical significance levels compared to the negative control is indicated by α ($p < 0.01$) and β ($p < 0.001$), while comparisons with the positive control is indicated by $^{***}p < 0.01$, $^{**}p < 0.02$ and $^{*}p < 0.05$.

Discussion

Natural products have been explored for several biomedical applications like amyloidosis (21, 22), antibacterial (23, 24), anticancer (19, 25), and cardiovascular diseases (26). Plant extracts like curcumin and aloe vera loaded with alginate gelatin hydrogel exhibited strong antioxidant properties, non-toxic, and reduced oxidative stress in the wound sites (27). Similarly, *Capparis sepiaria* combined with sodium alginate possessed antimicrobial, and anti-inflammatory properties and improved fluid absorption and tissue generation minimizing the infection and allergic reactions (28). Bassam *et al* enhanced healing by developing an eco-friendly gel formulation loaded with chitosan nanoparticles along with kiwi peels and yucca seeds. It is non-toxic, provides vitamins, antioxidants, and anti-inflammatory properties, and increases the entrapment efficacy, and bioavailability yielding better and rapid healing outcomes (29). Curcumin and rutin have also been explored for their potential for wound healing using antimicrobial assessment and antioxidant assay. The hydrogel containing these two active compounds exhibited higher wound-healing activity (30). Silk sericin, a natural protein obtained from silk fibers has been engineered as silk sponges to enable enhanced wound healing properties in a recent study (31). Banana stem extracts have shown rapid wound healing as evidenced by previous researchers (32). There are reports on exclusive wound-healing properties of banana extracts (33, 34). On the other hand, aloe vera has also progressed towards clinical trials for effective wound healing (35). Curcumin is a known anti-inflammatory agent and its nanoformulations have also been studied vastly for wound healing contributions (36, 37). We have selected these three phytochemicals, plantain peel extract, aloe vera extract, and curcumin along with nanosilver to study the enhanced efficacy of healing wounds compared to only silver. The combination of these phytochemicals has been entrapped in CMC hydrogel along with nanosilver.

CMC is a very well-known, biocompatible, and vastly used hydrogel used to design many therapeutic agents. Because these hydrogels were utilized as wound dressing material due to their versatile properties like absorption of wound exudate, barrier development, cell growth promotion, cell division, tissue respiration, and essential humidity, etc., CMC was used for exclusively wound dressing material support. CMC was derived from the polymer chitosan and possesses high biocompatibility, antibacterial, and solubility in water (38). Similarly, silver nanoparticles improve wound healing by inhibiting bacterial infections, decreasing the pain level, and increasing tissue regeneration (39). The combined hydrogel enhanced scar-free wound healing which was already proven (18). In this study, the hydrogels CMC@Ag and CMC@Ag+P were synthesized and characterized with different methods showing successful synthesis. The hydrogels were homogenous and highly stable. *In vivo* biocompatibility showed that the hydrogel CMC@

Ag+P, was biocompatible at both low and high doses, however, CMC@Ag showed mortality and abnormality at high doses. The cell migration or wound healing ability of both the hydrogels CMC@Ag and CMC@Ag+P was observed on the A375 cell line. Both the hydrogels resulted in enhanced cell migration. Compared to control and CMC@Ag, both the concentrations of CMC@Ag+P resulted in high cell migration even at 72 h proving the hydrogel's faster wound healing nature by rapid cell-cell communication and migration to cover the wound. Finally, we wanted to explore whether a rapid angiogenesis can happen at the wound site which can further accelerate the wound healing by supplying the nutrients at the wound site. Our angiogenesis assay supported the notion that our engineered hydrogel, CMC@Ag+P, could effectively induce angiogenesis compared to CMC@Ag and positive control, heparin. These findings altogether indicate that CMC@Ag+P can influence wound healing in a multifactorial way.

Conclusion

Burn wounds are one of the most unsafe wounds that affect every part of the body, and cause mental stress and even morbidity. Healing of burn wounds with non-toxicity is essential but accelerating to scar-free wound healing is more needed. Some ideal wound dressing material promotes wound healing along with scarring but specific natural compound blended wound dressing materials not only promotes wound healing but also increases the essential properties and promotes scar-free wound healing. The effective scar-free wound healing of both the hydrogels CMC@Ag and CMC@Ag+P was evaluated through *in vitro* cell migration assay, *in vivo* toxicity study, and CAM assay. Both formulations contributed to wound closure, although CMC@Ag+P demonstrated enhanced cell migration, and resulted in a pro-healing effect for superior wound closure activity. Likewise, the biocompatibility for both hydrogels was determined by the zebrafish toxicity study, where CMC@Ag+P showed minimal toxicity compared to CMC@Ag alone. Furthermore, the higher angiogenesis activity revealed by CMC@Ag+P indicates the increase in vascular growth that is crucial for wound healing. Furthermore, both the hydrogels contributed to wound closure, however, the CMC@Ag+P exhibited superior wound healing properties resulting in scar-free healing via higher angiogenesis, enhanced cell migration, and minimal toxicity. These further validate that the CMC@Ag+P is a promising biomaterial for advanced burn wound care management systems, associating both efficient recovery and enriched cosmetic outcomes.

Acknowledgement

The authors acknowledge Chettinad Academy of Research Institute for providing DJM, GJ, and SU with Ph.D. fellowship and the research infrastructure for carrying out the work.

Funding

This research received no external funding.

Conflict of Interest

The authors declare no conflicts of interest.

Ethical approval

The Ethical approval for the zebrafish embryo study was obtained from the Institution Animal Ethical Committee, Chettinad Academy of Research and Education (IAEC2/Proposal:118/A.Lr:90/Dt:16.09.2023).

Consent Statement

Not applicable.

Data Availability Statement

Data will be made available on request.

Author contributions

Devadass Jessy Mercy: Writing- original draft, Investigation and Data curation. **Gopalarethinam Janani:** Investigation, Data curation. **Saranya Udayakumar:** Investigation and data curation. **Agnishwar Girigoswami:** Writing – review & editing, Writing – original draft, Visualization, Validation, Supervision, Methodology, Investigation, Formal analysis, Data curation, Conceptualization**. Koyeli Girigoswami:** Writing – review & editing, Writing – original draft, Visualization, Validation, Supervision, Methodology, Investigation, Formal analysis, Data curation, Conceptualization**.**

References

1. Han S-K. Basics of Wound Healing. Innovations and Advances in Wound Healing. Singapore: Springer Nature Singapore; 2023. p. 1-42.
2. Jeschke MG, van Baar ME, Choudhry MA, Chung KK, Gibran NS, Logsetty S. Burn injury. Nature Reviews Disease Primers. 2020;6(1):11.
3. Kim H, Shin S, Han D. Review of History of Basic Principles of Burn Wound Management. Medicina. 2022;58(3):400.
4. Abazari M, Ghaffari A, Rashidzadeh H, Badeleh SM, Maleki Y. A Systematic Review on Classification, Identification, and Healing Process of Burn Wound Healing. The International Journal of Lower Extremity Wounds. 2022;21(1):18-30.
5. Oryan A, Alemzadeh E, Moshiri A. Burn wound healing: present concepts, treatment strategies and future directions. Journal of Wound Care. 2017;26(1):5-19.
6. Neagu TP, Tiglis M, Peride I, Lascar I. Factors involved in burn wound healing–short review. Romanian JouRnal of

medical PRactice. 2022;17(4):92.
7. Orbay H, Corcos AC, Ziembicki JA, Egro FM. Challenges in the Management of Large Burns. Clin Plast Surg. 2024;51(2):319-27.
8. Roberto López C, Carlos Rafael Hernández Á, Luis Alberto Salvador M, Victoria Méndez H, Amalia Ortiz V, Raúl Cristóbal de Jesús Rodríguez A, et al. Strategies for Wound Burn Healing. International Journal of Medical Science and Clinical Research Studies. 2024;4(12):2471-5.
9. Lestari T, Syukur S, Revilla G, Rita R, Rustini R. The Burn Wound Healing Process : A Review. International Journal of Progressive Sciences and Technologies. 2023;40:77.
10. Girard D, Laverdet B, Buhé V, Trouillas M, Ghazi K, Alexaline M, et al. Biotechnological Management of Skin Burn Injuries: Challenges and Perspectives in Wound Healing and Sensory Recovery. Tissue engineering Part B, Reviews. 2016;23.
11. Cohen-Gerassi D, BenShoshan M, Liiani A, Reuveni T, Loboda O, Haratz M, et al. Stable, Easy-to-Handle, Fully Autologous Electrospun Polymer-Peptide Skin Equivalent for Severe Burn Injuries. bioRxiv. 2025:2025.01. 12.632550.
12. Palaniraj S, Murugesan R, Narayan S. Aprotinin–Conjugated biocompatible porous nanocomposite for dentine remineralization and biofilm degradation. Journal of the Indian Chemical Society. 2022;99(10):100702.
13. Rashad AA, Ahmed A, Azmy O, Louis D. An overview on the application of nanotechnology in burn wound management. International Journal for Holistic Research. 2024:1-8.
14. Barkat H, Barkat MA, Ali R, Hadi H. Nanotechnological Advances in Burn Wound Care: Silver Sulfadiazine-Loaded Nanosuspension-Based Chitosan-Incorporated Nanogel for Partial Thickness Burns. Int J Low Extrem Wounds. 2025:15347346241309425.
15. Ijaz M, Khan M. Multifunctional electrospun nanofiber films of polyacrylonitrile and polyvinyl alcohol incorporating rhamnose and therapeutic agents for enhanced healing of infected burn wounds. J Biomater Sci Polym Ed. 2025:1-33.
16. Singh R, Kumar J, Rajput SK, Bhardwaj R, Ranjan G. Revolutionising shift in advanced wound healing therapies: nanoengineered herbal gels. Natural Product Research. 2024:1-16.
17. Capanema NSV, Mansur AAP, Carvalho SM, Mansur LL, Ramos CP, Lage AP, et al. Physicochemical properties and antimicrobial activity of biocompatible carboxymethylcellulose-silver nanoparticle hybrids for wound dressing and epidermal repair. Journal of Applied Polymer Science. 2018;135(6):45812.
18. Sharon Sofini PS, Mercy DJ, Raghavan V, Isaac JB, Deepika B, Udayakumar S, et al. Evaluation of scarless wound healing through nanohydrogel infused with selected plant extracts. Journal of Drug Delivery Science and Technology. 2024;100:106118.
19. Janani G, Girigoswami A, Deepika B, Udayakumar S, Mercy DJ, Girigoswami K. Dual Mechanism of Amphiroa anceps: Antiangiogenic and Anticancer Effects in Skin Cancer. Chemistry & biodiversity. 2025:e202500626.
20. Girigoswami A, Deepika B, Udayakumar S, Janani G, Mercy DJ, Girigoswami K. Peony-shaped zinc oxide nanoflower synthesized via hydrothermal route exhibits promising anticancer and anti-amyloid activity. BMC Pharmacology and Toxicology. 2024;25(1):101.
21. Girigoswami A, Ghosh M, Girigoswami K. World scenario of earthworms' prowess as a remedy to a spectrum of diseases–a glimpse on related nanoformulations. Tradit Med Res. 2025;10(4):23.
22. Metkar SK, Udayakumar S, Girigoswami A, Girigoswami K. Natural serine proteases and their applications in combating amyloid formation. ADMET and DMPK. 2024;12(6):797-820.
23. Rajkumar M, Davis Presley S, Thiyagarajulu N, Girigoswami K, Janani G, Kamaraj C, et al. Gelatin/PLA-loaded gold nanocomposites synthesis using Syzygium cumini fruit extract and their antioxidant, antibacterial, anti-inflammatory, antidiabetic and anti-Alzheimer's activities. Scientific Reports. 2025;15(1):2110.
24. Biswas K, Mercy DJ, Udayakumar S, Girigoswami A, Girigoswami K. Frustrating the Serenity of Bacterial Biofilms by Bristly Reduced Graphene Oxide Sheets. BioNanoScience. 2025;15(2):1-9.
25. Rajesh K, Priyadharshini R, Jayaraman S. Aloe emodin Inhibits Proliferation and Promotes Apoptosis in Non-Small Cell Lung Carcinoma (NSCLC) Cells by Deactivating PI3K/Akt/mTOR Signaling Pathways.
26. Sathishkumar K. Revitalising healthcare: the role of natural products in modern medicine. Natural Product Research. 2024:1-3.
27. Jessy Mercy D, Thirumalai A, Udayakumar S, Deepika B, Janani G, Girigoswami A, et al. Enhancing Wound Healing with Nanohydrogel-Entrapped Plant Extracts and Nanosilver: An In Vitro Investigation. Molecules. 2024;29(21):5004.
28. Ndlovu SP, Motaung KSCM, Adeyemi SA, Ubanako P, Ngema L, Fonkui TY, et al. Sodium alginate-based nanofibers loaded with Capparis Sepiaria plant extract for wound healing. Journal of Biomaterials Science, Polymer Edition. 2024;35(15):2380-401.
29. Bassam SM, Ali DE, Awwad ZM, Mahmoud SA, Abou-Taleb BA. Development and characterization of plant derived wastes Nano-formulation loaded in thermo-reversible gel for burn healing: An effort towards Sustainable Development. Journal of Drug Delivery Science and Technology. 2024;95:105543.
30. Keerthana B, John RS, Kumar M. Development of Photo-crosslinked Hydrogel incorporated with Curcumin/Rutin for Wound Healing: An Invitro Study. Library of Progress-Library Science, Information Technology & Computer. 2024;44(3).
31. Bhoopathy J, Sathyaraj WV, Prabakaran L, Senthil R,

Mohammed V, Dharmalingam S. An investigation on bioderived sponges with hemostatic and photoluminescent properties for accelerating wound healing. Journal of Polymers and the Environment. 2024;32(8):4005-16.
32. Amutha K, Selvakumari U. Wound healing activity of methanolic stem extract of Musa paradisiaca Linn. (Banana) in Wistar albino rats. International wound journal. 2016;13(5):763-7.
33. Agarwal P, Singh A, Gaurav K, Goel S, Khanna H, Goel R. Evaluation of wound healing activity of extracts of plantain banana (Musa sapientum var. paradisiaca) in rats. 2009.
34. Ekweogu CN, Akubugwo EI, Emmanuel O, Nosiri CI, Uche ME, Adurosakin OE, et al. Phytochemical profiling, toxicity studies, wound healing, analgesic and anti-inflammatory activities of Musa paradisiaca L. Musaceae (Plantain) stem extract in rats. Journal of Ethnopharmacology. 2024;322:117639.
35. Hekmatpou D, Mehrabi F, Rahzani K, Aminiyan A. The effect of aloe vera clinical trials on prevention and healing of skin wound: a systematic review. Iranian journal of medical sciences. 2019;44(1):1.
36. Kumari A, Raina N, Wahi A, Goh KW, Sharma P, Nagpal R, et al. Wound-healing effects of curcumin and its nanoformulations: a comprehensive review. Pharmaceutics. 2022;14(11):2288.
37. Akbik D, Ghadiri M, Chrzanowski W, Rohanizadeh R. Curcumin as a wound healing agent. Life sciences. 2014;116(1):1-7.
38. Gonçalves RC, Signini R, Rosa LM, Dias YSP, Vinaud MC, Lino Junior RS. Carboxymethyl chitosan hydrogel formulations enhance the healing process in experimental partial-thickness (second-degree) burn wound healing. Acta Cir Bras. 2021;36(3):e360303.
39. Singh M, Thakur V, Kumar V, Raj M, Gupta S, Devi N, et al. Silver Nanoparticles and Its Mechanistic Insight for Chronic Wound Healing: Review on Recent Progress. Molecules. 2022;27(17).